

Effect of the Yb substitutions on the thermoelectric properties of CaMnO_3

D. Flahaut¹, R. Funahashi^{1,2}, K. Lee³, H. Ohta^{3,4}, K. Koumoto^{3,4}

¹AIST, 1-8-31 Midorigaoka, Ikeda, Osaka 563-8577, Japan

²CREST, Japan Science and Technology Agency, Ikeda, Osaka 563-8577, Japan

³CREST, Japan Science and Technology Agency, 4-1-8 Honcho, Kawaguchi 332-0012, Japan

⁴Graduate School of Engineering, Nagoya University, Furo-cho, Chikusa-ku, Nagoya 464-8603 Japan

Fax: +81-72-751-9622, e-mail: delphine-flahaut@aist.go.jp

Abstract

$\text{Ca}_{1-x}\text{Yb}_x\text{MnO}_3$ ($x = 0-0.5$) samples were prepared via solid state reaction in air. Electrical and thermoelectric properties have been investigated up to 1000K. The measurements reveal that the resistivity values are strongly affected by the charge carrier content and the octahedral distortion. The lowest ρ reaches $3\text{m}\Omega\cdot\text{cm}$ for $x=0.15$. Whereas the Seebeck coefficient depends only on the charge carrier concentration, the thermal conductivity of $\text{Ca}_{1-x}\text{Yb}_x\text{MnO}_3$ is mainly governed by the mass difference between the Yb and Ca cations. The best ZT value, $\text{ZT}=0.2$, is obtained for $x=0.05$ at 1000K and demonstrates the good potentialities of these oxides as high temperature thermoelectric material.

Introduction

Thermoelectric generation systems can offer a reliable method to convert heat into electrical energy without detrimental waste. The materials, used in thermoelectric devices, have to fulfill a $\text{ZT}>1$ criterion, where Z is the figure of merit of thermoelectric conversion $Z = S^2/\rho\kappa$, with S the Seebeck coefficient, ρ the electrical resistivity and κ the thermal conductivity. Conventional materials, as metal chalcogenides [1,2] and Si-Ge alloys [3], reach this value but their thermal and chemical stability at high temperatures in air are not satisfying for thermoelectric conversion. Moreover, the materials must also be composed of non-toxic and abundantly available elemental materials. Therefore, the discovery of NaCo_2O_4 [4] with a large S ($100\mu\text{V}\cdot\text{K}^{-1}$) and low ρ ($0.2\text{m}\Omega\cdot\text{cm}$) at RT has motivated a renewed interest in new types of metal oxide materials [5]. Some p-type thermoelectric materials have been found, such as $\text{Ca}_3\text{Co}_4\text{O}_9$ ("349") [6], and $\text{Bi}_2\text{Sr}_2\text{Co}_2\text{O}_7$ [7]. Recently, Funahashi et al. [8] have built a thermoelectric device with high output power density. This module is composed of $\text{Ca}_{2.7}\text{Bi}_{0.3}\text{Co}_4\text{O}_9$ phase, as a p-type leg, and $\text{La}_{0.9}\text{Bi}_{0.1}\text{NiO}_3$ as n-type leg. The maximum output power obtained for this unicouple is 94 mW at 1073K ($\Delta T = 500\text{K}$). For instance, the 349 [6,9] phase remains the best p-type leg. On the other hand, the current n-type, $\text{La}_{0.9}\text{Bi}_{0.1}\text{NiO}_3$, although ρ is low ($1\text{m}\Omega\cdot\text{cm}$), is not suitable because of the too small absolute value of its Seebeck coefficient (around $-30\mu\text{V}\cdot\text{K}^{-1}$). To overcome the lack of good n-type, several studies of the CaMnO_3 perovskite have been made. These materials have first attracted attention for their properties of colossal magnetoresistance (CMR) and then they have also been suggested as potential n-type thermoelectric materials [9-12]. S value of CaMnO_3 is around $-350\mu\text{V}\cdot\text{K}^{-1}$ but its resistivity is too high ($\rho_{300\text{K}} = 2\Omega\cdot\text{cm}$). Consequently,

substitutions at the A- or B-site have been attempted to decrease the resistivity. By this way, a power factor, $\text{PF}=S^2/\rho$, of $0.3\text{mW}\cdot\text{m}^{-1}\text{K}^{-2}$ has been reached for $\text{CaMn}_{0.96}\text{Nb}_{0.4}\text{O}_3$ [11] and $0.28\text{mW}\cdot\text{m}^{-1}\text{K}^{-2}$ for $\text{Ca}_{0.9}\text{Bi}_{0.1}\text{MnO}_3$ at 1000K [13,14]. For these compounds, the value of |S| remains high (around $-100\mu\text{V}\cdot\text{K}^{-1}$) and much lower resistivity than that of CaMnO_3 was obtained.

In a previous paper [15], we reported on rare-earth substitutions at the A-site on the CaMnO_3 perovskite ($M = \text{Tb, Ho, Nb, Yb}$) reaching to a ZT enhancement. The best value $\text{ZT}=0.16$ at 1000K was obtained for $\text{Ca}_{0.9}\text{Yb}_{0.1}\text{MnO}_3$. Based on this fact, we were interested in the $\text{Ca}_{1-x}\text{Yb}_x\text{MnO}_3$ system. By varying the Yb^{3+} content, we address the role played by the different factors ($\langle r_A \rangle$, atomic weight, charge carrier) involved in the thermoelectric properties.

Experiment

Polycrystalline samples of $\text{Ca}_{1-x}\text{Yb}_x\text{MnO}_3$ ($x = 0-0.5$) were synthesized via solid state reaction in air. The compounds starting from stoichiometric mixtures of CaCO_3 , Mn_2O_3 and Yb_2O_3 were calcinated for 12h at 1073K, 1273K, and 1475K in air with intermediate grinding. Then the products were pressed into pellets, and sintered in air at 1573K for 15h. Finally, the pellets were cooled down to room temperature at the rate of $100^\circ\text{C}/\text{h}$ in the furnace.

X-ray powder diffraction (XRD) analysis was carried out with a Rigaku diffractometer using $\text{Cu-K}\alpha$ radiation for 2θ from 5° to 95° with an angle step of 0.01° . Lattice parameters were obtained from the Rietveld analysis of the X-ray data [16] by using the program Fullprof. The microstructures of the specimens were observed by a scanning electron microscopy (SEM) using both secondary electron and back-scattered electron modes. The constituent analysis was carried out by using an energy-dispersive X-ray spectrometer (EDX).

Resistivity measurements were performed by using a dc standard four-probe method in temperature range 300-1100K in air. The thermo-electromotive forces (ΔV) and temperature difference (ΔT) were measured at 373-973K and S was deduced from the relation $\Delta V/\Delta T$. Two Pt-Pt/Rh thermocouples were attached to both ends of the samples using silver paste. The Pt wires of the thermocouples were used for voltage terminals. Measured S values were reduced by those of Pt wires to obtain the net S values of the samples. Thermal conductivity κ is obtained from the thermal diffusivity, specific heat capacity and density. Thermal diffusivity and specific heat were measured by a laser flash method (ULVAC-TC3000V) and differential scanning calorimetry (MDSC2910, TA instruments), respectively in the temperature range from 373-973K with steps of 100K.

Results and discussion

The XRD patterns of $\text{CaMn}_{1-x}\text{Yb}_x\text{O}_3$ ($x=0$ to 0.5) are characteristic of an orthorhombic perovskite structure refined with the Pnma space group ($n^\circ 62$). Evolution of the unit cell volume versus both tolerance factor (t) and Yb^{3+} content, is plotted in Figure 1.

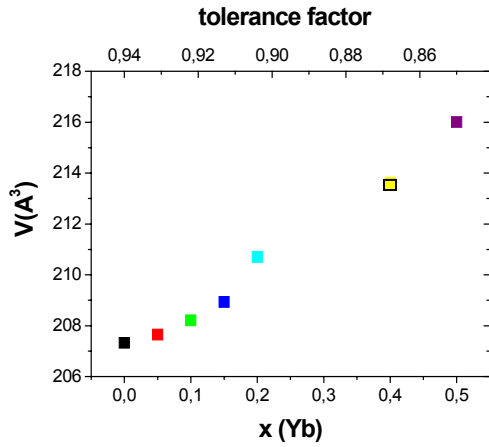


Figure 1: Cell volume evolution versus x and tolerance factor of $\text{CaMn}_{1-x}\text{Yb}_x\text{O}_3$.

The t parameter, which describes the geometric distortion of ABO_3 type perovskite is defined as $t = \frac{r_A + r_O}{\sqrt{2}(r_B + r_O)}$ [17]

where r_A , r_B , and r_O are the ionic radii of the atoms [18]. Although Yb^{3+} ionic radius (1.042 \AA) is smaller than that of Ca^{2+} (1.18 \AA), the cell volume increases linearly with the Yb^{3+} content. This is explained by the creation of Mn^{3+} cation (0.645 \AA) of which ionic radius is larger than that of Mn^{4+} (0.53 \AA). For perovskite, a $|t|$ value different from the unity indicates a non cubic cell: if $1 > t > 0.85$ the distortion induces a tetragonal structure, then for $t < 0.85$, the orthorhombic distortion takes place and finally for $t < 0.81$ the hexagonal structure appears. As well as the t decrease, the Mn-O-Mn angles get smaller whereas the Mn-O bond distances become larger.

The experimental average cationic compositions are found to be very close to the nominal one. Furthermore, the distribution of the Yb content does not indicate any tendency of phase separation (Table 1). A clear decrease of the grain size has also been observed as the Yb content increases.

x(Yb)	Ca	Yb	Mn
0.05	0.97	0.04	0.99
0.1	0.94	0.06	1
0.15	0.83	0.15	1.02
0.3	0.68	0.28	1.04
0.4	0.68	0.31	1.01
0.5	0.5	0.47	1.03

Table 1: Nominal and experimental composition of $\text{CaMn}_{1-x}\text{Yb}_x\text{O}_3$

For that system, the influence of the A-site cationic size and of the $\text{Mn}^{3+}/\text{Mn}^{4+}$ ratio in thermoelectrical properties must be studied.

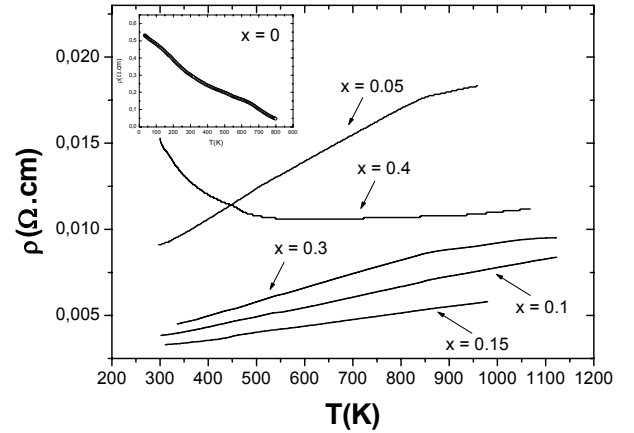


Figure 2: Resistivity as a function of temperature of $\text{CaMn}_{1-x}\text{Yb}_x\text{O}_3$.

The temperature dependence of the ρ of the samples is shown in Figure 2. The undoped CaMnO_3 is a n-type semiconductor which exhibits a ρ value around 0.3 \Omega.cm at room temperature. The Yb substitution decreases the resistivity in a spectacular way, according to the creation of Mn^{3+} charge carrier in the Mn^{4+} matrix. The evolution of ρ versus x passes by a minimum value for $x=0.15$, $3 \text{ m}\Omega.\text{cm}$ at 300K . First, for $x \leq 0.15$, the Yb substitution generates a strong decrease of the ρ values of two orders of magnitude accompanied by an insulating-metal transition. But, the resistivity increase for higher Yb content. One of the explanations is the influence of the $\langle r_A \rangle$ on the transport properties. In this system, the ionic radius of Yb (0.868 \AA) is much smaller than that of Ca (1.3 \AA), which contributes to the increase of octahedral distortion. This distortion is enhanced with Yb content and reduces the Mn-O-Mn bond angles. Consequently, the e_g electrons conduction bandwidth becomes narrower. For $x \leq 0.15$, this makes easier the electron conduction between e_g orbitals of the Mn^{3+} and Mn^{4+} cations. Thus, contrary to the hole-doped compounds, the resistivity decreases as the $\langle r_A \rangle$ and Mn-O-Mn bond angles decrease for n-type material [8]. No substituted CaMnO_3 systems possessing lower ρ than $\text{Ca}_{0.85}\text{Yb}_{0.15}\text{MnO}_3$, $3 \text{ m}\Omega.\text{cm}$ at 300K , have been reported [10-12]. Nonetheless, for $x > 0.15$, the narrowing of the e_g orbitals tends to localize the electrons and is responsible for the increase of the resistivity.

The purpose of this work is to enhance the ZT of CaMnO_3 compound. As Yb substitutions are effective in decreasing the resistivity, we hope to keep a relative high S value at high temperature.

In Figure 3, the evolution of S versus temperature for the CaMnO_3 and A-site doped compounds is shown. The negative S value confirms that the dominant electrical carriers are electrons for all the samples. The undoped compound CaMnO_3 shows a large absolute value of S which decreases as the temperature rises linked to its low carrier concentration and semiconductor behavior. S values are only affected by the $\text{Mn}^{3+}/\text{Mn}^{4+}$ ratio, so they evolve from -250 to $20 \mu\text{V.K}^{-1}$ at

1000K as Yb rises which is consistent with the increase of Mn^{3+} cations. Furthermore, the absolute S values increase with the temperature for substituted samples. Those S values have been compared to the theoretical one obtained from the

Heikes formula, $S = -\frac{k_B}{e} \ln\left(\frac{g_{Mn^{3+}} [Mn^{3+}]}{g_{Mn^{4+}} [Mn^{4+}]}\right)$. A good

agreement between both ($S_{th} = -273$ to $-20 \mu V.K$) was obtained which confirms the good stoichiometry of our samples.

To complete our analysis, thermal conductivity has been checked for the best samples.

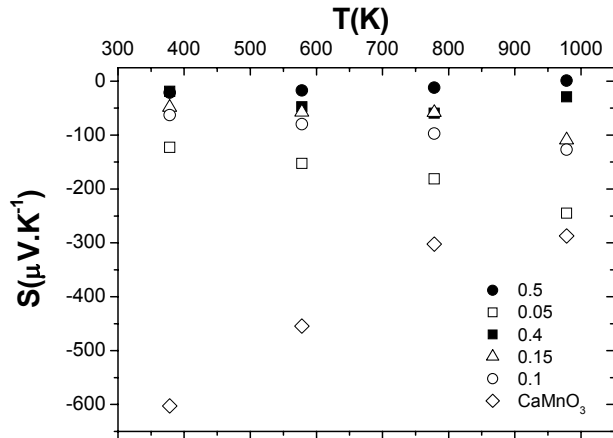


Figure 3: Temperature dependence of the Seebeck coefficient of $CaMn_{1-x}Yb_xO_3$ ($0 \leq x \leq 0.5$).

Figure 4 demonstrates the temperature dependence of the thermal conductivity of samples. The κ was calculated from the following formula $\kappa = DC_p d$, where D, C_p and d are the thermal diffusivity, the specific heat capacity and the density, respectively. For comparison, the data for the undoped $CaMnO_3$ from the work of Ohtaki et al. [11] is also plotted in this figure.

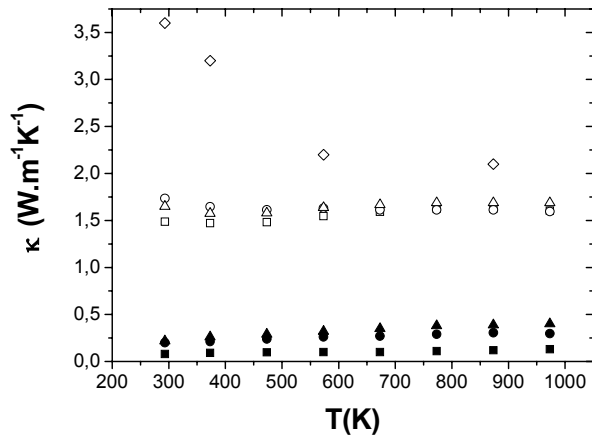


Figure 4: Temperature dependence of the thermal conductivity (κ) of $CaMn_{1-x}Yb_xO_3$ ($x = 0$ (diamond), 0.05 (open squares), 0.1 (open circles), 0.15 (open triangles)) and κ_l for closed symbols.

First of all, Yb substitutions decrease the κ comparing with $CaMnO_3$ sample. However, no considerable change is observed versus Yb content as observed in the $Ca_{1-x}Pr_xMnO_3$ system [19]. As ρ is very low ($<1 \Omega.cm$), the electronic contribution of κ has been calculated (Figure 4). κ can be expressed by the following formula $\kappa = \kappa_l + \kappa_e$, where κ_l is the lattice component and κ_e the electronic one. κ_e values are deduced from the Wiedemann-Franz's law $\kappa_e = LT\sigma$ ($L = 2.45 \cdot 10^{-8} W.\Omega.K^{-2}$). The κ_e values are negligible compared to κ_l . Nonetheless, they increase with Yb according to the increase of electronic conductivity. Thus, the κ decrease is mainly attributed to the distortion and the increase of the atomic weight of rare-earth, as reported in a previous paper [15]. Firstly, one can suggest that the mass difference between Yb and Ca atoms increases the lattice anharmonicity and thus the phonon-phonon interaction. On the other hand, the decrease of the bond angles, which conducts the octahedral distortion, also plays a role in the κ values. The decrease of the grain size with x has also to be taken into account in the decrease of the κ_l .

Thus, in those compounds, the thermal conductivity mainly depends on the atomic weight difference of the A-site, and to a lesser extent to the $\langle r_A \rangle$. So, doping with a heavy and small Re^{3+} minimizes the phonon component of the thermal conductivity. By this way, a higher figure of merit could be obtained in these perovskite oxides.

A compromise between, high S, low ρ and κ , is obtained for Yb 0.05. The ZT value obtained at 1000K reaches 0.2. The substitution of Ca by 5% of Yb is sufficient to enhance by a factor 4 the ZT at 1000K of $CaMnO_3$. Unfortunately, Z decreases for higher Yb content according to the strong decrease of the Seebeck coefficient. This value is much higher than those previously reported for $Ca_{0.9}Bi_{0.1}MnO_3$ (ZT=0.08) [13] and $Ca_{0.9}Y_{0.1}MnO_{2.97}$ (ZT=0.16) [14].

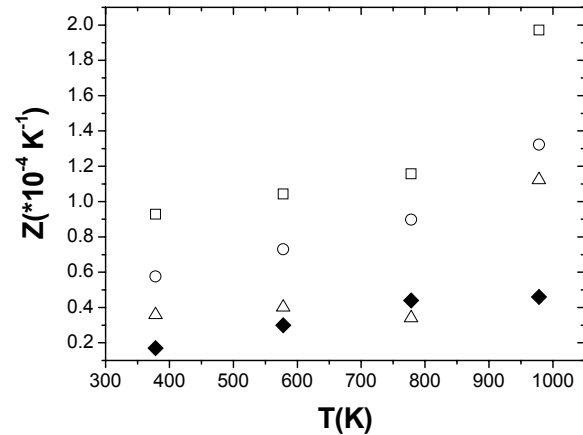


Figure 5: Z versus temperature of $CaMn_{1-x}Yb_xO_3$ ($x = 0$ (diamond), 0.05 (open squares), 0.1 (open circles), 0.15 (open triangles)).

Conclusions

The $\text{CaMn}_{1-x}\text{Yb}_x\text{O}_3$ ($0 \leq x \leq 0.5$) series crystallize in the orthorhombic perovskite with the Pnma space group. It was shown that electrical properties are mainly governed by the electron carrier and octahedral distortion. Yb substitutions are a good way to decrease the phonon contribution to the thermal conductivity which is directly linked to the distortion and atomic weight difference on the Ca-site. By this way, a high ZT can be obtained in CaMnO_3 system. Now, we plan to build bulk module with the $\text{Ca}_{0.95}\text{Yb}_{0.05}\text{MnO}_3$ compound as a n-type.

Acknowledgments

D. Flahaut acknowledges the Japan Society for the Promotion of Science for awarding her the Foreigner Postdoctoral Fellowship (ID P05864).

References

1. J. F. Nakahara, T. Takeshita, M. J. Tschetter, B. J. Beaudry, K. A. Gshneider Jr., *J. Appl. Phys.* 63 (1998) 2331.
2. A. Boyer, E. Cisse, *Mater. Sci. Eng.*, B 113 (1992) 103.
3. G. A. Slack, M. A. Hussain, *J. Appl. Phys.* 70 (1991) 3694.
4. I. Terasaki, Y. Sasago, K. Uchinokura, *Phys. Rev. B* 56, R12685 (1997).
5. S. Li, R. Funahashi, I. Matsubara, K. Ueno, H. Yamada, *J. Mater. Chem.* 9 (1999) 1659 ; T. Okuda, K. Nakamishi, S. Miyasaka, Y. Tokura, *Phys. Rev. B* 63 (2001) 113104.
6. A. C. Masset, C. Michel, A. Maignan, M. Hervieu, O. Toulemonde, F. Studer, B. Raveau, J. Hejtmanek, *Phys. Rev. B* 62 (2000) 166-175.
7. R. Funahashi, M. Shikano, *Appl. Phys. Lett.* 81 (2002) 1459.
8. R. Funahashi, S. Urata, K. Mizuno, T. Kouuchi, M. Mikami., *Appl. Phys. Lett.*, 85 (2004) 1036; R. Funahashi, T. Mihara, M. Mikami, S. Urata, N. Ando, *Proc. 24th Int. Conf. Thermoelectrics* p 292.
9. G. Xu, R. Funahashi, I. Matsubara, M. Shikano, Y. Zhou, *J. Mater. Res.* 17, 1092 (2002).
10. A. Maignan, S. Hébert, Li. Pi, D. Pelloquin, C. Martin, C. Michel, M. Hervieu, B. Raveau, *Crystal Eng.* 5 (2002) 365.
11. G. Xu, R. Funahashi, Q. Pu, B. Liu, R. Tao, G. Wang, Z. Ding, *Solid State Ionics* 174 (2004) 147.
12. S. Hashimoto, H. Iwahara, *Mater. Res. Bull.* 35, 2253 (2000).
13. M. Ohtaki, H. Koga, T. Tokunaga, K. Eguchi, H. Arai, *J. Solid State Chem.* 120, 105 (1995).
14. T. Kobayashi, H. Takizawa, T. Endo, T. Sato, H. Taguchi, M. Nagao, *J. Solid State Chem.* 92, 116 (1991).
15. D. Flahaut et al., *J. Appl. Phys.*, submitted.
16. J. Rodriguez-Carvajal, *Physica B* 195, 55 (1993).
17. V. M. Goldschmidt, *Akad. Oslo I, Mat.-Natur.*, No 2, 7 (1926).
18. R. D. Shannon, *Acta Cryst. A* 32 (1976) 751.
19. B. C. Cong, T. Tsuji, P. X. Thao, P. Q. Thanh, Y. Yamamura, *Physica B* 352 (2004) 18.